# Soft modes, Gaps and Magnetization Plateaus in 1D Spin-1/2 Antiferromagnetic Heisenberg Models

A. Fledderjohann, C. Gerhardt, M. Karbach, K.-H. Mütter and R. Wießner
*Physics Department, University of Wuppertal, 42097 Wuppertal, Germany*
(February 1, 2008-v2.2)

We study the one-dimensional spin-1/2 model with nearest and next-to-nearest-neighbor couplings exposed to a homogeneous magnetic field $h_3$ and a dimer field with period $q$ and strength $\delta$. The latter generates a magnetization plateau at $M = (1 - q/\pi)/2$, which evolves with strength $\delta$ of the perturbation as $\delta^\epsilon$, where $\epsilon = \epsilon(h_3, \alpha)$ is related to the $\eta$-exponent which describes the critical behavior of the dimer structure factor, if the perturbation is switched of ($\delta = 0$). We also discuss the appearance of magnetization plateaus in ladder systems with $l$ legs.

## I. INTRODUCTION

The existence or nonexistence of a gap between the energies of the ground state and the low lying excited states is the most important criterium for the criticality of a quantum spin system. Haldane's conjecture[1,2] states that one-dimensional (1D) quantum spin systems have no gap for half integer spin $s$, but do have a gap for integer spin $s$. The conjecture only holds for an appropriate choice of the couplings of the spins at nearest neighbor sites.[3]

The Lieb, Schultz, Mattis (LSM) construction[4,5] allows rigorous statements on the degeneracy of the ground state. Starting from the unitary operator

$$\mathbf{U} \equiv \exp\left(-i\frac{2\pi}{N}\sum_{l=1}^{N} l S_l^3\right), \tag{1.1}$$

it is straightforward to prove that the application of the operator $\mathbf{U}^k,\ k = 1, 2, ...$ on the ground state $|0\rangle$ generates *new* states

$$|k\rangle \equiv \mathbf{U}^k|0\rangle \quad k = 1, 2, \ldots;\ k \text{ finite}, \tag{1.2}$$

with an energy expectation value

$$\langle k|\mathbf{H}|k\rangle - \langle 0|\mathbf{H}|0\rangle = O(N^{-1}) \tag{1.3}$$

approaching the ground state energy $E_0 \equiv \langle 0|\mathbf{H}|0\rangle$ in the thermodynamical limit $N \to \infty$.

Of course the crucial question is whether the *new* states $|k\rangle$ are different from the ground state $|0\rangle$ or not. This question can be answered by an analysis of the quantum numbers of the states $|k\rangle,\ k = 1, 2, \ldots$. For example in the case of the Spin-1/2 Hamiltonian with nearest neighbor couplings:

$$\mathbf{H}(h_3) \equiv 2\sum_{l=1}^{N} \mathbf{S}_l \cdot \mathbf{S}_{l+1} - 2h_3\mathbf{S}_3(0), \tag{1.4}$$

and

$$\mathbf{S}_a(q) \equiv \sum_{l=1}^{N} e^{iql} S_l^a, \quad a = 1, 2, 3, \tag{1.5}$$

the ground state has momentum $p_s = 0, \pi$ and the total Spin $S_T^3 = S = NM(h_3)$, where $M$ is the magnetization. The new states $|k\rangle$ turn out to be eigenstates of the translation operator $\mathbf{T}$:

$$\mathbf{T}|k\rangle = \mathbf{T}\mathbf{U}^k|0\rangle = e^{ip_k}|k\rangle, \tag{1.6}$$

where[6]

$$p_k = p_s + kq_3(M), \tag{1.7}$$

and $q_3(M) \equiv \pi(1 - 2M)$. For $M = 0$ the ground state $|0\rangle$ and the new state $|1\rangle$ differ in their momenta by $\pi$ and are therefore orthogonal to each other.
For $M = 1/4$ one finds a fourfold degeneracy of the ground state with momenta $p_k = p_s + k\pi/2,\ k = 0, 1, 2, 3$.

It should be noted that the LSM construction allows to identify the zero frequency excitations (soft modes) in the model with Hamiltonian (1.4). Some of these soft modes induce characteristic signatures, e.g. zeroes in the dispersion curve and singularities in the transverse and longitudinal structure factors at the soft mode momenta $q = q_1(M) \equiv \pi,\ q = q_3(M)$, which can be easily recognized even on rather small systems.[7] Following conformal field theory the corresponding critical $\eta$-exponents can be determined from the finite-size behavior of the dispersion curve at the soft mode momenta.[8] It is known that the $\eta$-exponents of the soft mode – i.e. the $M$ dependence of $\eta_3(M), \eta_1(M)$ – changes,[9] if we add further couplings to the Hamiltonian (1.4). In some cases (see the discussion below) the soft mode might disappear completely and a gap opens between the states, which were gapless before switching on the perturbation.

The following cases (A.-E.) have been studied so far.

### A. A transverse staggered field

A gap was found[10−12] in a transverse staggered field of strength $h_1\mathbf{S}_1(\pi)$,

$$\mathbf{H}(h_3, h_1) \equiv \mathbf{H}(h_3) + 2h_1\mathbf{S}_1(\pi), \tag{1.8}$$

between the states which differ in their momenta by $\pi$. Indeed the operator $\mathbf{S}_1(\pi)$ is invariant only under translations $\mathbf{T}^2$ and the eigenstates of the Hamiltonian are only eigenstates of $\mathbf{T}^2$.

In the free field case ($h_3 = 0$) the $\mathbf{T}^2$ quantum numbers of the ground state $|0\rangle$ and of the LSM state $|1\rangle = \mathbf{U}|0\rangle$ are the same and the twofold degeneracy of the ground state is lifted by the explicit breaking of translation invariance.

The fourfold degeneracy with momenta $p=0,\pi,\pm\pi/2$ which occurs at $M = 1/4$ and $h_1 = 0$ is lifted in the following manner. The states with $p = 0$ and $p = \pi$ are even with respect to $\mathbf{T}^2$. The same holds for the ground state $|0\rangle$, which is a linear combination of $p = 0$ and $p = \pi$ components. A gap opens to the second state, which is even under $\mathbf{T}^2$. The gap evolves with the strength $h_1$ of the perturbation as $h_1^\epsilon$. The exponent $\epsilon = \epsilon_1(h_3)$ is given by the exponent $\eta_1(M)$

$$\epsilon_1(h_3) = 2[4 - \eta_1(M(h_3))]^{-1}, \tag{1.9}$$

associated with the divergence of the transverse structure factor at $q = \pi$.

The LSM construction with the operator (1.1) leads to a second state $|1\rangle = \mathbf{U}|0\rangle$ which is degenerate with the ground state $|0\rangle$ and which is odd under $\mathbf{T}^2$. This state can be constructed as a linear combination of momentum eigenstates with $p = \pm\pi/2$.

### B. A longitudinal periodic field

A longitudinal periodic field $\bar{\mathbf{S}}_3(q)$ of strength $2h_q$

$$\mathbf{H}(h_3, h_q) \equiv \mathbf{H}(h_3) + 2h_q\bar{\mathbf{S}}_3(q), \tag{1.10}$$

with

$$\bar{\mathbf{S}}_3(q) \equiv [\mathbf{S}_3(q) + \mathbf{S}_3(-q)]/2, \tag{1.11}$$

induces a plateau in the magnetization curve $M = M(h_3)$ at $M = (1 - q/\pi)/2$, i.e. $q$ has to meet the soft mode momentum $q = q_3(M)$. The difference of the upper and lower critical field:

$$\Delta(h_q, h_3) \equiv h_3^u - h_3^l \sim h_q^{\epsilon_3(h_3)}, \tag{1.12}$$

evolves with an exponent, which is again related via (1.9) to the corresponding $\eta_3$-exponent and which can be extracted from the finite-size behavior of the longitudinal structure factor[8] at $q = q_3(M)$.

### C. A next-to-nearest-neighbor coupling

A next-to-nearest-neighbor coupling

$$\mathbf{H}_2 \equiv 2\sum_{l=1}^{N} \mathbf{S}_l \cdot \mathbf{S}_{l+2}, \tag{1.13}$$

added to Hamiltonian (1.4):

$$\mathbf{H}(h_3, \alpha) \equiv \mathbf{H}(h_3) + \alpha\mathbf{H}_2, \tag{1.14}$$

does not change the position of the soft modes $q_1 = \pi$ and $q_3(M)$ but changes the associated $\eta_1(M,\alpha)$, $\eta_3(M,\alpha)$ exponents.[9] A singlet triplet gap opens in the free field case ($h_3 = 0$) for $\alpha > \alpha_c = 0.241\ldots$.[13] Note, however, that (1.13) is translation invariant and therefore the ground state degeneracy with momenta $p = 0,\pi$ – predicted by the LSM construction – still holds, i.e. the singlet ground state is still twofold degenerate in the singlet sector.

### D. A staggered dimer field

A plateau in the magnetization curve at $M = 1/4$ has been found in the Hamiltonian (1.4) with an additional next-to-nearest-neighbor coupling and a staggered dimer field:[14,15]

$$\mathbf{H}(h_3, \alpha, \delta) \equiv \mathbf{H}(h_3) + \alpha\mathbf{H}_2 + \delta\mathbf{D}(\pi). \tag{1.15}$$

The dimer operator is defined as:

$$\mathbf{D}(q) \equiv 2\sum_{l=1}^{N} e^{iql}\mathbf{S}_l \cdot \mathbf{S}_{l+1}. \tag{1.16}$$

Such a Hamiltonian only commutes with $\mathbf{T}^2$ and therefore reduces the degeneracy of the ground state. At $M = 0$ the twofold degeneracy of the ground state is lifted and a gap opens between the energies of the ground state and the excited states.[10]

At $M = 1/4$ a gap opens between the ground state $|0\rangle$ and one further state, which is even under $\mathbf{T}^2$. The LSM construction yields a second state $|1\rangle = \mathbf{U}|0\rangle$ degenerate with the ground state $|0\rangle$, which is odd under $\mathbf{T}^2$.

### E. A periodic dimer field

A plateau in the magnetization curve at $M = 1/6$ has been found[16] for a Hamiltonian of the type (1.4) with a dimer field $\bar{\mathbf{D}}(q)$ of period $q = 2\pi/3$:

$$\bar{\mathbf{D}}(q) \equiv [\mathbf{D}(q) + \mathbf{D}(-q)]/2. \tag{1.17}$$

The Hamiltonian used in Ref. 16 can be reformulated as a single spin-1/2 chain with ferromagnetic nearest neighbor coupling being strongly disturbed by an antiferromagnetic next-to-nearest neighbor coupling with a period of $q = 2\pi/3$.

Note, that the periodicity $q = 2\pi/3$ coincides with the soft mode momentum $q_3(M = 1/6)$. Such a coincidence occurs in both examples I B and I E and we conclude that the special type of the periodic perturbation (1.11) and (1.17) is not relevant for the formation of a magnetization plateau.

The situation in example I D is different. Here the periodicity ($q = \pi$) of the staggered dimer field coincides with the *second soft mode* $2q_3(M = 1/4) = \pi$ [ (1.7) for $k = 2$], predicted by the LSM construction. Note, however, that the magnetization plateau at $M = 1/4$ is only visible if the parameters $\alpha$ and $\delta$ in (1.15) are appropriately chosen. In particular the magnetization plateau at $M = 1/4$ seems to be absent if the next-to-nearest-neighbor coupling $\alpha$ is switched off. Therefore, we conclude that the coincidence of the periodicity $q$ in the perturbation operator with the momentum of one LSM-soft mode is a necessary – but not sufficient – condition for the formation of a plateau.

It is the purpose of this paper to investigate in more detail the mechanism for the formation of gaps and magnetization plateaus by means of periodic dimer-perturbations (1.17) of strength $2\delta_q$. The $\delta_q$-evolution of the energy eigenvalues and transition matrix elements of the perturbation operator is given by a closed set of differential equations, which we have discussed in Refs. 10,11. The initial values for these evolution equations are given by the energy eigenvalues and transition amplitudes for the unperturbed case ($\delta_q = 0$).

The outline of the paper is as follows. In Sec. II we complete the discussion of the quantum numbers of the LSM state $|k\rangle$ by investigating their $\mathbf{S}_T^2$ content, where $\mathbf{S}_T$ is the total spin operator. We are in particular interested in the question, whether or not the LSM state $|1\rangle$ at $M = 0$ with momentum $p_1 = p_0 + \pi$ contains a triplet ($S = 1$) or higher spin component [$\mathbf{S}_T^2 = S(S + 1)$]. Section III is devoted to an analysis of the LSM soft modes in the dimer-dimer structure factor. This analysis is used to fix the above mentioned initial conditions for the evolution equations. In Sec. IV we then present numerical results on the formation of gaps and plateaus by means of the periodic dimer perturbations.

The occurrence of magnetization plateaus in spin ladders is discussed in Sec. V.

## II. THE LIEB, SCHULTZ, MATTIS (LSM) CONSTRUCTION AND THE QUANTUM NUMBERS OF THE DEGENERATE GROUND STATES.

It has been pointed out in the introduction that the quantum number analysis of the states $|k\rangle = \mathbf{U}^k|0\rangle$ in the LSM construction is crucial to decide whether these states are new, i.e. orthogonal to the ground state $|0\rangle$, or not. The transformation behavior (1.6) under translations $\mathbf{T}$ yields the momenta $p_k$ (1.7) of these states.

The operator $\mathbf{U}$ (1.1) obviously commutes with the total spin in 3-direction $S_T^3$. Therefore all the states $|k\rangle = \mathbf{U}^k|0\rangle$ have the same total Spin $S_T^3$ in 3-direction. The Hamiltonian of type (1.14) with isotropic couplings commutes with $\mathbf{S}_T^2$. One might ask for the $\mathbf{S}_T^2$ content of the states $|k\rangle$. To answer this question we compute the expectation value

$$\begin{aligned}\langle k|\mathbf{S}_T^2|k\rangle - \langle 0|\mathbf{S}_T^2|0\rangle &= \langle 0|\mathbf{U}^{\dagger k}\mathbf{S}_T^2\mathbf{U}^k|0\rangle - \langle 0|\mathbf{S}_T^2|0\rangle \\ &= 2N[S_1(q = k2\pi/N, M) - S_1(0, M)], \end{aligned} \quad (2.1)$$

using the considerations developed by LSM to show the vanishing of the energy difference (1.3). The right-hand side of (2.1) is determined by the transverse structure factor, exposed to an external field $h_3$ with magnetization $M(h_3)$:

$$S_1(q, M) \equiv \sum_{l=1}^{N} e^{iql}\langle S, p_s|S_1^1 S_{1+l}^1|S, p_s\rangle, \quad (2.2)$$

which has been studied on finite systems in Ref. 17 for the nearest neighbor model (1.4) and in Ref. 18 for the model with next-to-nearest-neighbor couplings $\alpha$.

From these investigations we conclude for the thermodynamical limit of the difference appearing on the right-hand side of (2.1):

$$2N[S_1(k2\pi/N, M) - S_1(0, M)] \overset{N\to\infty}{\longrightarrow} A(M)\left(\frac{2\pi}{N}\right)^{\beta_k}. \quad (2.3)$$

The exponent $\beta_k = \beta_k(M, \alpha)$ turns out to be zero for $M = 0$ and $\alpha = 0$ [cf. Fig. 5(d) in Ref. 17]. This means, that the right-hand side of (2.1) is non vanishing. For $M = 0, \alpha = 0$ the ground state is a singlet state [$\mathbf{S}_T^2 = S(S + 1) = 0$] and (2.1) tells us that the soft mode state $|k = 1\rangle = \mathbf{U}|0\rangle$ with momentum $\pi$ contains triplet [$\mathbf{S}_T^2 = S(S + 1) = 2$] and higher spin components, i.e. the LSM construction together with (2.3) and $\beta_k(M = 0, \alpha = 0) = 0$ forbids a singlet triplet gap.

The exponent $\beta_k(M, \alpha)$ is larger than zero for $M > 0$ [cf. Inset of Fig. 5(b) in Ref. 7] In this case the right-hand side of (2.1) vanishes and the soft mode states $|k\rangle = \mathbf{U}^k|0\rangle$ have the same total spin $\mathbf{S}_T^2 = S(S + 1)$ as the ground state.

Switching on the next-to-nearest-neighbor coupling $\alpha$ the free field exponent must be larger than zero

$$\beta_1(0, \alpha) > 0 \quad \text{for} \quad \alpha > \alpha_c = 0.241\ldots, \quad (2.4)$$

since the dimer phase $\alpha > \alpha_c$ is characterized by a singlet triplet gap.[13] In other words, for $\alpha > \alpha_c$ the degenerate LSM state $|1\rangle = \mathbf{U}|0\rangle$ with momentum $p_s + \pi$ must be a pure singlet state as well. The exponent $\beta_1(0, 1/2)$ can easily be calculated at the Majumdar-Ghosh[19,20] point $\alpha = 1/2$ . Here we find $\beta_1(0, 1/2) = 1$.

In Fig. 1 we have plotted the energy difference $\omega_\pi = E_1 - E_0$ of the two singlet states $|0\rangle$ and $|1\rangle$

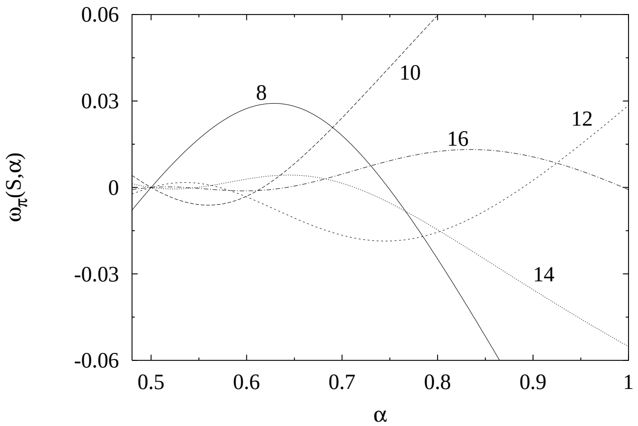


FIG. 1. The energy differences (2.5) for system sizes $N = 8, 10, \ldots, 16$ and $S = 0$.

$$\omega_\pi(S=0,\alpha) = E(p_s+\pi, S=0,\alpha) - E(p_s, S=0,\alpha), \tag{2.5}$$

versus the coupling $\alpha$. This is an oscillating function for $\alpha > 0.5$ with zeroes at:

$$\alpha = \alpha_1(N) < \alpha_2(N) < \ldots < \alpha_Z(N), \tag{2.6}$$

where numerical data suggest that the total number of zeroes is given by

$$Z = \frac{1}{4}\begin{cases} N & : N = 8, 12, 16, \ldots \\ N-2 & : N = 10, 14, 18, \ldots . \end{cases} \tag{2.7}$$

In the thermodynamical limit we have a dense distribution of zeroes. The height of the maxima and minima in between converges to zero – a signal for the degeneracy of the two states $|0\rangle$ and $|1\rangle = \mathbf{U}|0\rangle$ in the thermodynamical limit as predicted by the LSM construction.

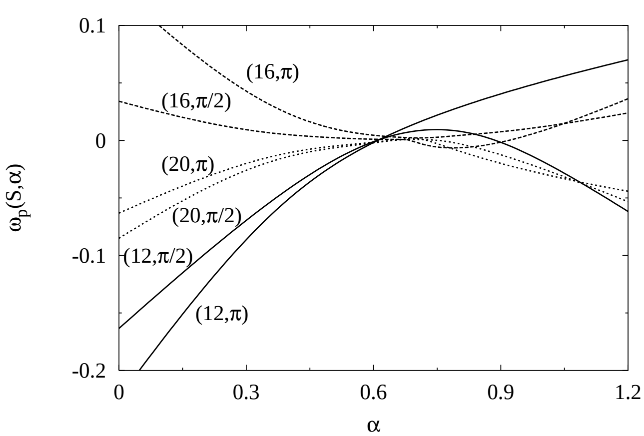


FIG. 2. The energy differences (2.8) for system sizes $N = 8, 12, 16$ and momentum $p = \pi, \pi/2$ and $S = N/4$. Same line types denote the same system sizes.

As was pointed out in the introduction, a fourfold degeneracy of the states $|k\rangle = \mathbf{U}^k|0\rangle$, $(k = 0, 1, 2, 3)$ is predicted at $M = 1/4$. All these states have the same total spin squared ($S = N/4$) and momenta $p = 0, \pm\pi/2, \pi$. On finite systems one again observes oscillations in the energy differences

$$\omega_p(S,\alpha) \equiv E(p, S = N/4, \alpha) - E(0, S = N/4, \alpha), \tag{2.8}$$

for $p = \pi/2, \pi$, if we switch on the next-to-nearest-neighbor coupling $\alpha$ as is shown in Fig. 2. For $\alpha$ values large enough these oscillations die out and the ground state momentum $p_s, S = N/4$ is supposed to be

$$p_s(1/4) = \frac{\pi}{2}\begin{cases} 2 & : N = 8, 24, 40, \ldots \\ 1 & : N = 12, 28, 44, \ldots \\ 0 & : N = 16, 32, 48, \ldots \\ 1 & : N = 20, 36, 52, \ldots . \end{cases} \tag{2.9}$$

## III. SOFT MODES IN THE DIMER DIMER STRUCTURE FACTOR

According to the LSM construction for the translation invariant models with nearest and next-to-nearest-neighbor couplings (1.14), $\mathbf{H}(h_3, \alpha)$, we expect the dispersion curve

$$\omega_q(S,\alpha) \equiv E(p_s+q, S, \alpha) - E(p_s, S, \alpha), \tag{3.1}$$

to develop zeroes

$$\omega^{(k)}(h_3,\alpha) \equiv \omega_q(S,\alpha), \tag{3.2}$$

at the soft mode momenta $q = q^{(k)}(M) \equiv k\pi(1-2M)$. If in the thermodynamical limit the scaled energy differences:

$$\hat{\Omega}^{(k)}(M,\alpha) \equiv \lim_{N\to\infty} N\omega^{(k)}(h_3,\alpha). \tag{3.3}$$

and

$$v(M,\alpha) = \lim_{N\to\infty} N[E(p_s+2\pi/N, S, \alpha) - E(p_s, S, \alpha)], \tag{3.4}$$

are finite and non vanishing, the ratios

$$\eta^{(k)}(M,\alpha) \equiv \frac{\hat{\Omega}^{(k)}(M,\alpha)}{\pi v(M,\alpha)}, \tag{3.5}$$

yield the exponents $\eta^{(k)}(M,\alpha)$, which govern the critical behavior of the dimer dimer structure factor:

$$S_{DD}(q,M) = \frac{1}{N}\langle p_s, S|\mathbf{D}_c(q)\mathbf{D}_c^\dagger(q)|p_s, S\rangle. \tag{3.6}$$

Here

$$\mathbf{D}_c(q) \equiv \mathbf{D}(q) - \delta_{q0}\mathbf{D}(0)$$

is the connected part of the dimer operator (1.16). For $M=0$ a zero should occur at $q=\pi$ and for $M=1/4$ we should find two zeroes at $q=\pi/2$ and $q=\pi$. This is indeed the case as can be seen from Fig. 3 where we have plotted the dispersion curves for $M=1/4$, $\alpha=0,1/4$.

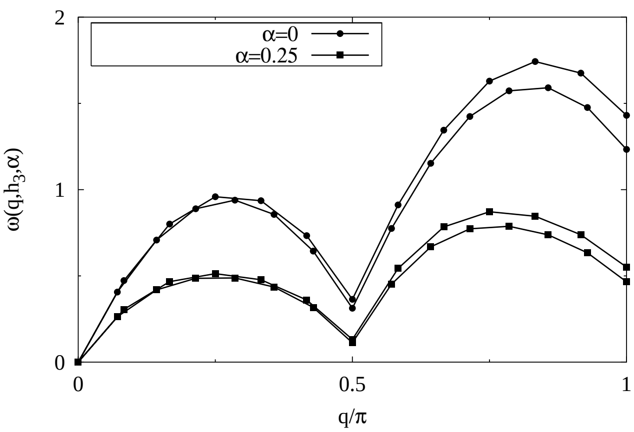


FIG. 3. The dispersion curve of the Hamiltonian (1.14) for finite system ($N=24,28$) and magnetization $M=1/4$.

Note, that the dimer operator commutes with the total Spin $\mathbf{S}_T^2$ and the dispersion curve (3.1) describes the lowest lying excitations contributing to $S_{DD}(q,M,\alpha)$.

The $q$-dependence of the dimer-dimer structure factor (3.6) at $M=1/4$ and $\alpha=0,1/4$ is shown in Fig. 4. A pronounced peak is found at the first soft mode $q=\pi(1-2M)=\pi/2$. The finite-size behavior of the structure factor at the first soft mode

$$S_{DD}(q_3(M),M,\alpha)\sim N^{1-\eta_3(M,\alpha)} \tag{3.7}$$

is shown for $\alpha=0,1/4$ and $M=1/4$ in the inset of Fig. 4. It is well described by an exponent

$$\eta^{(1)}(1/4,\alpha)=\eta_3(1/4,\alpha)=\begin{cases}1.53 & :\alpha=0\\ 0.72 & :\alpha=1/4.\end{cases} \tag{3.8}$$

identical with the exponent $\eta_3(M,\alpha)$ in the longitudinal structure factor. The latter has been calculated exactly in the model with nearest neighbor couplings ($\alpha=0$) by means of Bethe ansatz solutions for the energy eigenvalues, which enter in the differences (3.1) and (3.4). The resulting curve $\eta_3(M,\alpha=0)$ is shown in Fig. 2 of Ref. 8. The $\alpha$-dependence of $\eta_3(1/4,\alpha)$ has been calculated on small systems ($N\leq 28$) and can be seen in Fig. 4(b) of Ref. 9.

According to its definition (3.6), the dimer dimer structure factor can be represented:

$$S_{DD}(q,M,\alpha)\equiv\frac{1}{N}\sum_n|\langle n|\mathbf{D}_c(q)|0\rangle|^2 \tag{3.9}$$

in terms of transition amplitudes from the ground state $|0\rangle=|p_s,S\rangle$ to excited states $|n\rangle$ with momenta $p_n=p_s+q$ and total spin $S$. The peak in Fig.4 tells us that the transition matrix elements at the first soft mode $q=\pi(1-2M)$

$$\langle n|\mathbf{D}(\pi(1-2M))|0\rangle\overset{N\to\infty}{\longrightarrow}N^{\kappa_3}, \tag{3.10}$$

with $\kappa_3=1-\eta_3(M(h_3),\alpha)/2$, diverge with the system size.

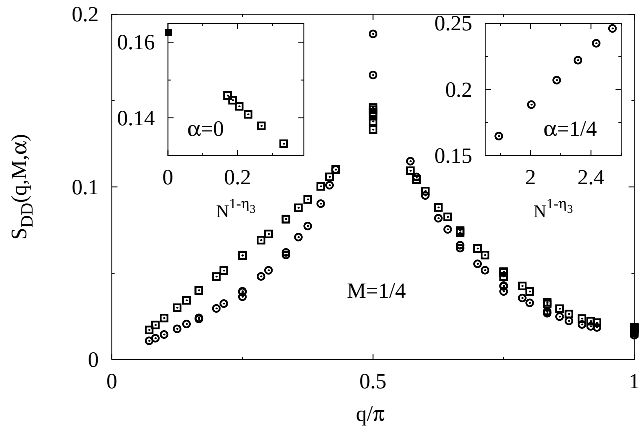


FIG. 4. The dimer dimer structure factor (3.9) at $M=1/4$ for $N=12,16,\ldots,28$. The insets show the $N$-dependence of the structure factor $S_{DD}$ at $q=\pi/2$, versus $N^{1-\eta_3}$, with exponent $\eta_3$ given by Eq. (3.8). For $\alpha=1/4$ the structure factor diverges and for $\alpha=0$ it is finite. The extrapolated value ($N\to\infty$) is marked with a solid symbol (■).

The fact, that there is no peak at the second soft mode, indicates that the corresponding transition matrix elements $\langle n|\bar{\mathbf{D}}(q=2\pi(1-2M))|0\rangle$ are small – at least for next-to-nearest-neighbor couplings $\alpha\leq 1/4$. The magnitude of these transition matrix elements is crucial for the formation of gaps and magnetization plateaus with a periodic perturbation $\bar{\mathbf{D}}(q)$.

## IV. PERIODIC DIMER PERTURBATIONS AND THE FORMATION OF GAPS AND PLATEAUS

In this section we will study the impact of a periodic dimer perturbation $\bar{\mathbf{D}}(q)$ (1.17):

$$\mathbf{H}(h_3,\alpha,\delta_q)\equiv\mathbf{H}(h_3,\alpha)+2\delta_q\bar{\mathbf{D}}(q), \tag{4.1}$$

on the soft modes. We will restrict ourselves to the model with nearest neighbor and next-to-nearest-neighbor couplings and follow the procedure of Refs. 10,11. There it was shown that the $\delta_q$-evolution of the energy eigenvalues and transition matrix elements $\langle n|\bar{\mathbf{D}}(q)|0\rangle$ is described by a closed set of differential equations which possess finite size scaling solutions in the limit $N\to\infty$, $\delta_q\to 0$, $x=\delta_q^\epsilon N$ fixed.

This statement holds, if the periodicity $q$ of the dimer perturbation coincides with a soft mode momentum:

$$q = q^{(k)}(M) = k\pi(1-2M). \tag{4.2}$$

Then a gap in the energy difference (3.1) between the ground state and lowest state which can be reached with the perturbation $\bar{\mathbf{D}}(q)$ at $q^{(k)}(M)$ is predicted:

$$\omega^{(k)}(h_3,\alpha,\delta_q) = \delta_q^{\epsilon^{(k)}}\Omega^{(k)}(M,\alpha,x). \tag{4.3}$$

The gap opens with an exponent $\epsilon^{(k)} = \epsilon^{(k)}(h_3,\alpha)$, related to the corresponding $\eta$-exponent (3.5) via

$$\epsilon^{(k)}(h_3,\alpha) = 2[4-\eta^{(k)}(M(h_3),\alpha)]^{-1}. \tag{4.4}$$

A test of the prediction (4.3) is given in Fig. 5, where we plotted the gap ratio

$$\frac{\omega^{(1)}(h_3,\alpha,\delta_q)}{\omega^{(1)}(h_3,\alpha,0)} = 1 + e^{(1)}(h_3,\alpha,x), \tag{4.5}$$

for $M = 1/4$, i.e. $q = \pi/2$ and $\alpha = 0, 1/4$ versus the scaling variable $x^{2/\epsilon}$ with the exponents

$$\epsilon = \epsilon^{(1)}(1/4,\alpha) = \begin{cases} 0.81(1) & : \alpha = 0 \\ 0.64(3) & : \alpha = 1/4 \end{cases} \tag{4.6}$$

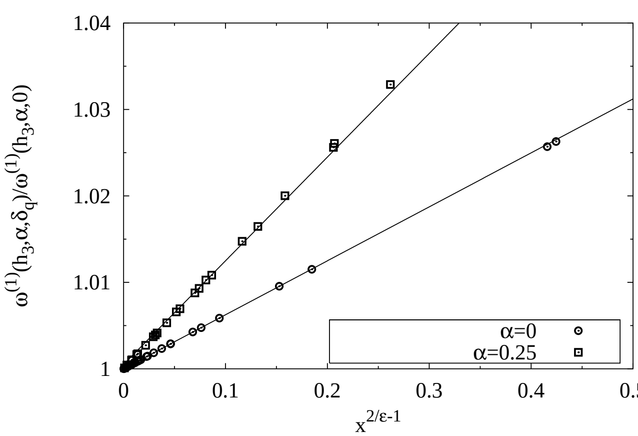


FIG. 5. The gap ratio (4.5) versus the scaling variable $(N\delta^{\epsilon})^{2/\epsilon-1}$, with $\epsilon$ given by Eq. (4.6). The solid lines represent linear fits to the small $x$-behavior.

Note that the gap ratio (4.5) is linear in $x^{2/\epsilon}$ for small values of $x$, as predicted by the evolution equations for the scaling functions.[10,11]

Let us next study the influence of the periodic perturbation (1.17) on the magnetization curve $M = M(h_3)$. A plateau in the magnetization curve with an upper and lower critical field $h_3^u$ and $h_3^l$ will emerge if

$$\Delta(\delta_q,h_3) \equiv h_3^u - h_3^l = \lim_{N\to\infty}\left[E(p_{s+1},S+1,\alpha,\delta_q) + E(p_{s-1},S-1,\alpha,\delta_q) - 2E(p_s,S,\alpha,\delta_q)\right], \tag{4.7}$$

does not vanish in the thermodynamical limit, i.e. if the ground state energies $E(p_{s'},S',\alpha,\delta_q)$ for $S' = S-1, S, S+1$ evolve in a different manner under the perturbation $\delta_q$. This happens exactly if the periodicity $q$ of the dimer perturbation coincides with a soft mode momentum (4.2). Then the ground state energy at the 'critical' magnetization $M = S_T^3/N$ is lowered stronger than at the neighboring magnetizations $M = (S_T^3 \pm 1)/N$.

In Fig. 6 we show the $\delta_q$-evolution of the magnetization curves for $q = \pi/2$ and $\alpha = 1/4$. The emergence of the predicted plateau at $M = 1/4$ is clearly visible.

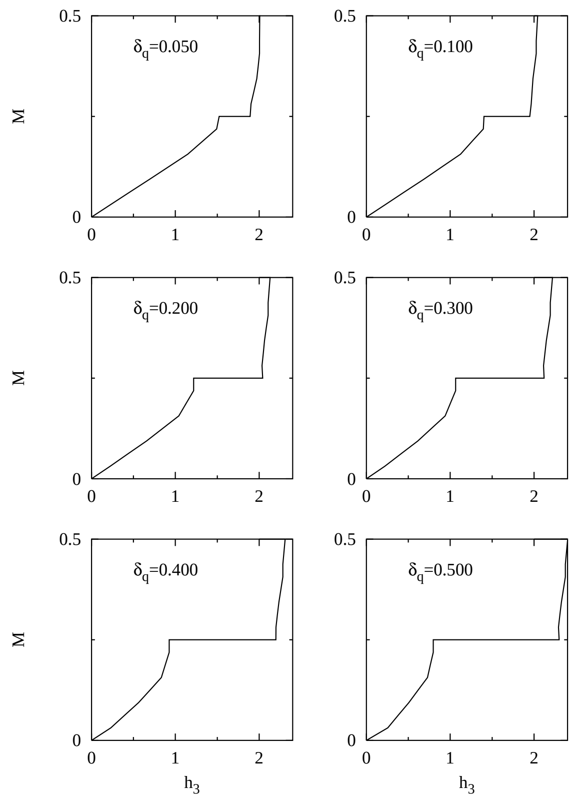


FIG. 6. The magnetization curve of $\mathbf{H}(h_3,\alpha,\delta_q)$ for $\alpha = 0.25$ and different $\delta_q$-values, determined from finite system sizes $N = 8, 12, 16, 20$.

The scaling behavior $\delta_q^{\epsilon}$ with $\epsilon = \epsilon^{(1)}(h_3,\alpha)$ of the difference (4.7) is governed by the critical exponent $\eta^{(1)}(h_3,\alpha)$ at $h_3 = h_3(M = 1/4)$ of the unperturbed model at the first soft mode $q_3(M)$ as can be seen in Fig. 7.

We also looked for the $\delta$-evolution of the magnetization curves for a dimer perturbation with periodicity $q = \pi$. There is a plateau for $M = 0$ – corresponding to the gap above the ground state discussed in Ref. 9. However, no plateau is visible at $M = 1/4$ for small perturbations $\delta\mathbf{D}(\pi)$. This corresponds to the observation that the second soft mode at $M = 1/4$, $q = \pi$, does not produce any signature in the dimer dimer structure factor.

These statements only hold for small perturbations $\delta\mathbf{D}(\pi)$. It is indeed known from Refs. 14,15 that a plateau

at $M = 1/4$ can be enforced with a large perturbation of order 1.

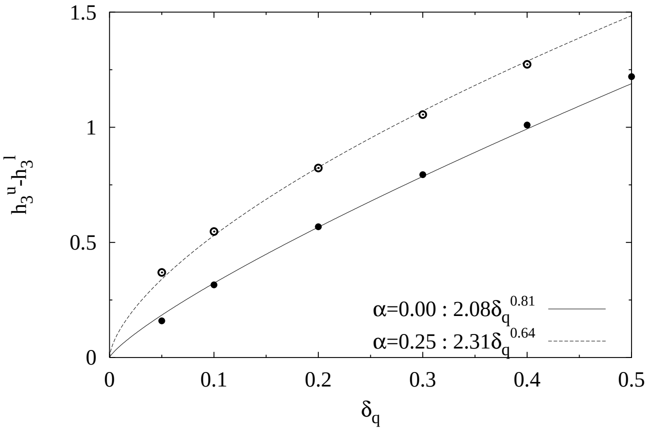


FIG. 7. The evolution of the difference (4.7) between the upper and lower critical field at the plateau $M = 1/4$. The dotted and dashed line show a fit, proportional to $\delta_q^\epsilon$ with $\epsilon = \epsilon^{(1)}$ given by Eq. (4.6), to small values of the external field $\delta_q$.

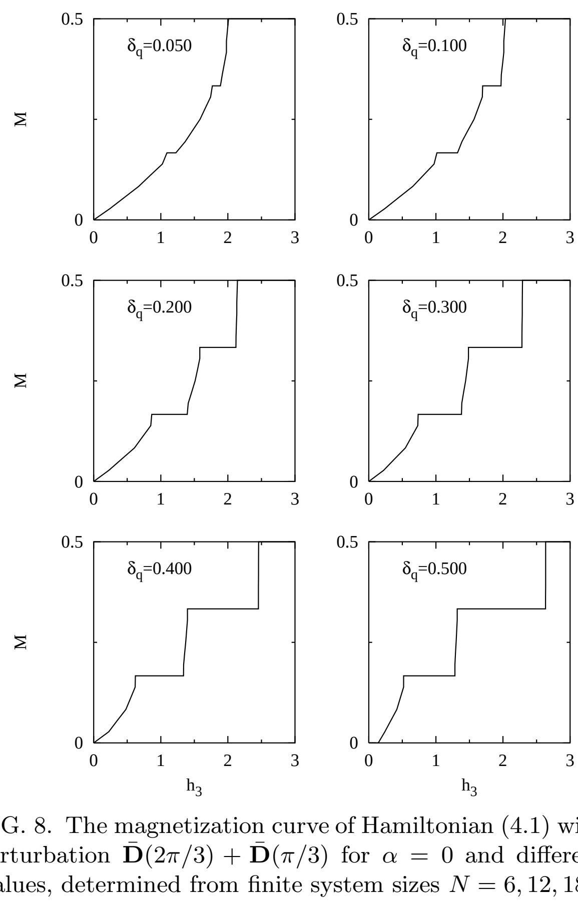


FIG. 8. The magnetization curve of Hamiltonian (4.1) with a perturbation $\bar{\mathbf{D}}(2\pi/3) + \bar{\mathbf{D}}(\pi/3)$ for $\alpha = 0$ and different $\delta_q$-values, determined from finite system sizes $N = 6, 12, 18$.

We have computed magnetization curves for the Hamiltonian (4.1) with perturbations $\bar{\mathbf{D}}(q)$ of period $q = 2\pi/3$ and $q = \pi/3$. We found clear evidence for the expected magnetization plateaus at $M = 1/6$ and $M = 1/3$. The magnetization curve for a Hamiltonian with a superposition of both perturbations

$$\bar{\mathbf{D}}(2\pi/3) + \bar{\mathbf{D}}(\pi/3), \tag{4.8}$$

is shown in Fig. 8. Here, we find two plateaus in the magnetization curve at $M = 1/6$ and $M = 1/3$.

## V. MAGNETIZATION PLATEAUS IN SPIN LADDERS

All the considerations we made so far for the 1D Hamiltonian (4.1) with nearest and next-to-nearest-neighbor couplings can be extended to the case

$$\mathbf{H}(h_3, \alpha_l) \equiv \mathbf{H}(h_3) + \alpha_l \mathbf{H}_l, \tag{5.1}$$

where we substitute the next-to-nearest-neighbor coupling by couplings over $l$ lattice spacings

$$\mathbf{H}_l \equiv 2 \sum_{n=1}^{N} \mathbf{S}_n \cdot \mathbf{S}_{n+l}. \tag{5.2}$$

For $l$ finite the position $q_3(M)$ of the first soft mode – generated by the LSM construction – will not change, the corresponding $\eta$-exponent might change. According to our experience with the case $l = 2$, we expect that a slightly frustrating coupling enhances the singularity in the dimer dimer structure factor at $q = q_3(M)$. Hamiltonians of the type (5.1) are interesting, since they can be viewed as a spin ladder system with $l$ legs, as is shown in Fig. 9.

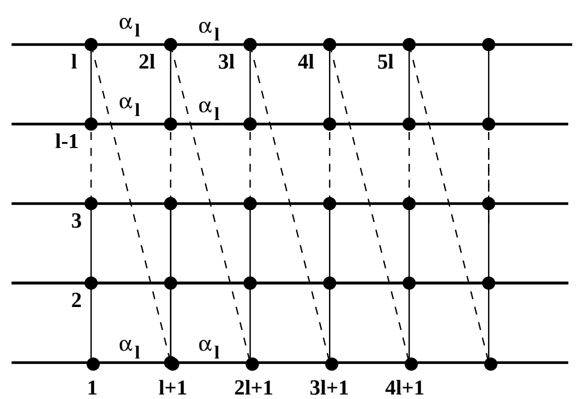


FIG. 9. A spin ladder system described by Hamiltonian (5.1) with $l$ legs, and additional diagonal couplings (dashed lines). The coupling strength between the legs is one unit.

They differ, however, from usual spin ladder systems with $l$ legs, owing to the diagonal (dashed) couplings $[(l \leftrightarrow l+1), (2l \leftrightarrow 2l+1), \dots]$, which are inferred by the helical boundary conditions.

Indeed, these additional couplings change the physical properties. Spin ladder systems with helical boundary conditions are gapless – irrespective of the number of legs. This statement holds if the couplings $\alpha_l$ along the legs is chosen properly, e.g. the two leg system with $l = 2$ is gapless for $\alpha \le \alpha_c = 0.241\dots$. Conventional ladder systems are known to be gapless for an odd number of legs, but to be gapped for an even number of legs.

This fundamental difference becomes clear, when we add a special dimer field to (5.1)

$$\mathbf{D}^{(l)} \equiv \sum_{n=1}^{N} J_n^{(l)} \mathbf{S}_n \cdot \mathbf{S}_{n+1}, \tag{5.3}$$

which only affects the diagonal couplings $[(l \leftrightarrow l+1), (2l \leftrightarrow 2l+1), \dots]$, in Fig. 9:

$$J_n^{(l)} = \begin{cases} 0 & : n = 1, \dots, l-1 \\ \delta & : n = l, \end{cases} \tag{5.4}$$

$$J_{n+l}^{(l)} = J_n^{(l)}. \tag{5.5}$$

The periodicity (5.5) of the couplings $J_n^{(l)}$ is given by a Fourier series

$$J_n^{(l)} = \sum_{j=0}^{[l/2]} \cos(2\pi n j/l)\delta(q = 2\pi j/l), \tag{5.6}$$

where $[l/2]$ is the largest integer smaller than $l/2$. The Fourier coefficients $\delta(q)$ follow from (5.4), e.g. for $l = 2$ we find:

$$\delta(q = 0) = \delta(q = \pi) = \delta/2. \tag{5.7}$$

The dimer perturbation:

$$\delta\mathbf{D}^{(2)} = \frac{\delta}{2}[\mathbf{D}(0) + \mathbf{D}(\pi)] \tag{5.8}$$

generates a plateau at $M = (1 - q/\pi)/2 = 0$. Therefore, the gap – typical for the two leg ladder – appears immediately if we switch on the dimer field (5.3), which breaks the translation invariance of the 1D system.

Let us next consider the three leg ladder ($l = 3$). The Fourier coefficients turn out to be

$$\delta(q = 0) = \frac{c_3}{1 + c_3}\delta, \quad \delta(q = 2\pi/3) = \frac{1}{1 + c_3}\delta, \tag{5.9}$$

with $c_3 = \cos(\pi/3)$. The $q = 2\pi/3$ component in the dimer field (5.3):

$$\delta\mathbf{D}^{(3)} = \delta(q = 0)\mathbf{D}(0) + \delta(q = 2\pi/3)\mathbf{D}(2\pi/3), \tag{5.10}$$

generates a plateau at $M = 1/6$. This is exactly the plateau found in Ref. 21.

Note, that the Fourier decomposition of $\delta\mathbf{D}^{(l)}$ contains in general a $q = \pi$ component for even $l$ and no $q = \pi$ component for odd $l$. We therefore find a gap at $M = 0$ for ladders with an even number of legs but no gap for ladders with an odd number of legs.

In summary we can say, the Fourier decomposition of the dimer field (5.3)

$$\delta\mathbf{D}^{(l)} = \sum_{j=0}^{[l/2]} \delta(q = 2\pi j/l)\mathbf{D}(q = 2\pi j/l), \tag{5.11}$$

tells us, where to expect plateaus in the magnetization curve of a spin ladder system with $l$ legs. The position of plateaus can be seen in Table I.

The number of plateaus increases with the number of legs and one is tempted to suggest that in the two dimensional limit $l \to \infty$, the magnetization curve is again a continuous function. It should be noted, however, that the LSM-construction with the operator (1.1) breaks down in the combined limit $N \to \infty$, $k = \sqrt{N}$ in the sense that (1.3) does not hold.

The magnetic properties of the two dimensional Heisenberg model with helical boundary conditions at $T = 0$ have been studied in Ref. 22. Concerning the isotropic model with nearest neighbour coupling, there is no indication for a plateau in the magnetization curve.

Finally, let us mention that there is a second way to map ladder systems with $l$ legs onto one-dimensional systems with far reaching couplings:

$$\mathbf{H}(h_3, \tau_l) \equiv \mathbf{H}(h_3) + \tau_l \mathbf{H}_{N/l}. \tag{5.12}$$

The couplings for the $l$ leg system are shown in Fig. 10,

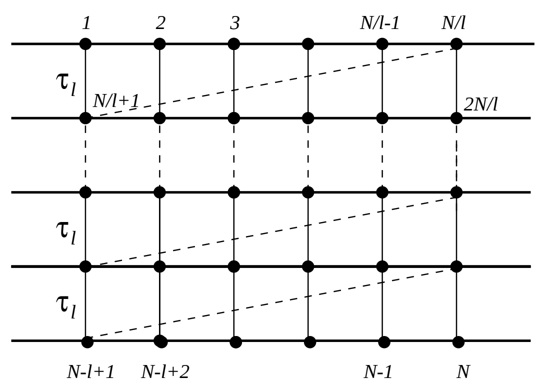


FIG. 10. Spin ladder system with $l$ legs described by Hamiltonian $\mathbf{H}(h_3, \tau_l)$ [Eq. (5.12)].

and for the two leg system in Fig. 11,

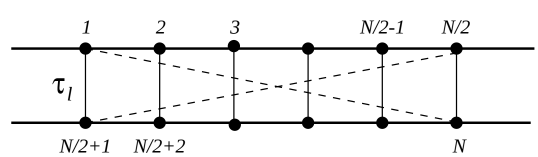


FIG. 11. Spin ladder system with two legs described by Hamiltonian $\mathbf{H}(h_3, \tau_2)$.

The latter differs from the conventional two leg system (with periodic boundary-conditions) only by a twist at the boundary, which should not change the physical properties in the thermodynamical limit. Therefore, we expect a gap in this system. The appearance of a gap in the systems with an even number $l$ of legs originates from the second term in the Hamiltonian (5.12). If we repeat the calculation of the expectation values (1.3) for the Hamiltonian (5.12) we find:

$$\langle k|\mathbf{H}|k\rangle - \langle 0|\mathbf{H}|0\rangle = O(N^{-1})$$
$$+\sum_{n=1}^{N}\left(\langle 0|\mathbf{U}^k \mathbf{S}_n \mathbf{S}_{n+N/l} \mathbf{U}^{\dagger^k} - \mathbf{S}_n \mathbf{S}_{n+N/l}|0\rangle\right) =$$
$$\sum_{n=1}^{N} f_l^k \langle 0|\mathbf{S}_n^+ \mathbf{S}_{n+N/l}^- + \mathbf{S}_n^- \mathbf{S}_{n+N/l}^+|0\rangle + O(N^{-1}). \quad (5.13)$$

The coefficient $f_l^k = [\cos(2\pi k/l) - 1]\tau_l$ does not vanish unless

$$k = l, 2l, \ldots . \quad (5.14)$$

This means in particular that the LSM-operators $\mathbf{U}^k$, $k = 1, \ldots, l-1$ do not create states, which are degenerate with the ground state in the thermodynamical limit.

Those situations, where the ground state degeneracy is lifted completely, are of special interest. They occur if the momenta of the states $|l\rangle = \mathbf{U}^l|0\rangle$ $[p_l = l\pi(1-2M) + p_s]$ and of the ground state $|0\rangle$ $(p_s)$ differ by a multiple of $2\pi$, i.e. for

$$\frac{l}{2}(1-2M) \in \mathbb{Z}. \quad (5.15)$$

The condition (5.15) is satisfied exactly for the $l$ and $M$ values, listed in Table I, i.e. for those values, where we expect a plateau in the magnetization curve.

## VI. CONCLUSION AND PERSPECTIVES

In this paper we tried to elucidate the mechanism which generates gaps and plateaus in spin 1/2 antiferromagnetic Heisenberg models with nearest and next to nearest neighbor couplings of strength $\alpha$. A priori these models have no gap in the presence of a homogeneous field $h_3 > h_3^c(\alpha)$ above the critical field $h_3^c(\alpha)$, which is needed to surmount the singlet triplet gap for $\alpha > \alpha_c = 0.241\ldots$. The LSM construction predicts the existence of soft modes (zero energy excitations) at wave vectors $q^{(k)}(M) = k\pi(1-2M),\ k = 1, 2, 3, \ldots$.

It is shown in Sec. II that the total spin squared $\mathbf{S}_T^2 = S(S+1)$ of the lowest excited states at the soft mode momenta is the same as that of the ground state for $S = MN$. The soft modes are therefore expected to generate signatures in the dimer dimer structure factor, since the dimer operator does not change the total spin squared.

Indeed, for $M = 1/4$ a pronounced peak is seen at the first soft mode $q = q^{(1)}(1/4) = \pi/2$ if $\alpha \leq 1/4$, indicating a large transition matrix element $\langle 1|\bar{\mathbf{D}}(\pi/2)|0\rangle$ between the ground state – with momentum $p_s$ – and the first excited state with momentum $p_s + \pi/2$.

The second soft mode $q = q^{(2)}(1/4) = \pi$, however, does not produce any visible structure in the dimer dimer structure factor (for $\alpha \leq 0.25$). Here the relevant transition matrix elements $\langle 1|\mathbf{D}(\pi)|0\rangle$ between the ground state $|0\rangle$ and the first excited state with momentum $p_s+\pi$ are small. The situation is different for large next-to-nearest-neighbor couplings $\alpha$.

The magnitude of the transition matrix elements $\langle 1|\bar{\mathbf{D}}(q)|0\rangle$ is crucial for the efficiency of the mechanism to generate a plateau in the magnetization curve at a rational value of $M$ by means of a periodic perturbation $\delta_q\bar{\mathbf{D}}(q)$. According to the criterium of Oshikawa, Yamanaka and Affleck[6] a plateau at $M$ is possible if $q$ meets one of the soft modes $q = q^{(k)}(M),\ k = 1, 2, 3, \ldots$.

Our numerical analysis shows that the width of the plateau – i.e. the difference of the upper and lower critical field (4.7) – depends on the magnitude of the transition matrix element in the unperturbed model ($\delta_q = 0$). Indeed these matrix elements enter as initial conditions in the differential equations [(2.4),(2.5)] and [(2.2),(2.3)] in Refs. 10,11, which describe the evolution of gaps and plateaus under the influence of a periodic perturbation $\delta_q\bar{\mathbf{D}}(q)$. We have also demonstrated that a superposition of two periodic perturbations $[\bar{\mathbf{D}}(2\pi/3) + \bar{\mathbf{D}}(\pi/3)]$ generates two plateaus in the magnetization curve exactly at those magnetization values ($M = 1/6, 1/3$) where the period ($q = 2\pi/3, \pi/3$) in the perturbation coincides with the first soft mode momentum $q = q_3(M)$.

Ladder systems with $l$ legs [cf. Fig. 9] can be interpreted as one-dimensional systems with additional couplings over $l$ lattice spacings and a dimerized perturbation (5.3) and (5.4). The latter breaks translation invariance of the 1D system and the Fourier analysis (5.11) of the dimerized perturbation (5.3) reveals the occurrence of magnetization plateaus [cf. Tab. I] in spin ladder systems with $l$ legs.

In this paper we concentrated our investigations on different spin-1/2 systems that all had in common that they reduce in the unperturbed case to critical Heisenberg chains. It should be pointed out that there exist exact solutions on other (multichain spin-1/2 antiferromagnetic Heisenberg-like) models,[23] where the existence of magnetization plateaus is still unclear. We remark that the application of the method we presented here, is not limited to the cases we discussed. However, besides looking for the existence of soft modes it turns out to be needed to discuss the strength of the transition matrix elements. Here, we cannot offer general prescription and therefore the dynamics of each different model of interest has to be treated separately.

## ACKNOWLEDGMENTS

We would like to thank A. Honecker and A. Klümper for discussions.



[1] F. D. M. Haldane, Phys. Lett. **93A**, 464 (1983).
[2] F. D. M. Haldane, Phys. Rev. Lett. **50**, 1153 (1983).
[3] K.-H. Mütter, Z. Phys. B **96**, 105 (1994).
[4] E. Lieb, T. Schulz, and D. Mattis, Ann. Phys. **16**, 407 (1961).
[5] I. Affleck and E. Lieb, Lett. Math. Phys. **12**, 57 (1986).
[6] M. Oshikawa, M. Yamanaka, and I. Affleck, Phys. Rev. Lett. **78**, 1984 (1997).
[7] M. Karbach, K.-H. Mütter, and M. Schmidt, J. Phys.: Condens. Matter **7**, 2829 (1995).
[8] A. Fledderjohann *et al.*, Phys. Rev. B **54**, 7168 (1996).
[9] C. Gerhardt *et al.*, J. Phys.: Condens. Matter **9**, 3435 (1997).
[10] A. Fledderjohann, M. Karbach, and K.-H. Mütter, to be published in Euro. Phys. J. B, (1998).
[11] A. Fledderjohann, M. Karbach, and K.-H. Mütter, submitted to Euro. Phys. J. B.
[12] M. Oshikawa and I. Affleck, Phys. Rev. Lett. **79**, 2883 (1997).
[13] K. Okamoto and K. Nomura, Phys. Lett. A **169**, 433 (1992).
[14] T. Tonegawa, T. Nishida, and M. Kaburagi, to be published in Physica B, (1998).
[15] K. Totsuka, Phys. Rev. B **57**, 3454 (1998).
[16] K. Hida, J. Phys. Soc. Jpn. **63**, 2359 (1994).
[17] M. Karbach, K.-H. Mütter, and M. Schmidt, Phys. Rev. B **50**, 9281 (1994).
[18] M. Schmidt, C. Gerhardt, K.-H. Mütter, and M. Karbach, J. Phys.: Condens. Matter **8**, 553 (1996).
[19] C. K. Majumdar and D. K. Ghosh, J. Math. Phys. **10**, 1388 (1969).
[20] C. K. Majumdar and D. K. Ghosh, J. Math. Phys. **10**, 1399 (1969).
[21] D. Cabra, A. Honecker, and P. Pujol, Phys. Rev. Lett. **79**, 5126 (1997).
[22] M.-S. Yang and K.-H. Mütter, Z. Phys. B **104**, 117 (1997).
[23] V. Y. Popkov and A. A. Zvyagin, Phys. Lett. **A 175**, 295 (1993); A. A. Zvyagin, Phys. Rev. B **51**, 12579 (1995); A. A. Zvyagin, Phys. Rev. B **57**, 1035 (1998).


| $l$ | 2 | 3 | 4 | 5 | 6 |
|---|---|---|---|---|---|
| $M$ | 0 | 1/6 | 0;1/4 | 1/10;3/10 | 0;1/6;1/3 |

TABLE I. The possible position of plateaus for spin ladders (5.1) with $l$ legs.